Determination of Optimum Thickness of Corner Bracket Considering Buckling and/or Plastic Collapse†

Yukio UEDA* and Tetsuya YAO**

Abstract

A method is proposed to determine the optimum thickness of a corner bracket in relation to the buckling and/or plastic strength. The fundamental idea of the proposed method is that the collapses of a frame and a bracket take place at the same time, since it is of no use for a bracket to carry more loads after the frame has collapsed. The determined thickness of a bracket is confirmed to be optimum by performing a series of elastic-plastic large deflection analyses by the finite element method.

KEY WORDS: (Optimum Thickness) (Buckling) (Plastic Collapse) (Corner Bracket) (Stress Distribution) (Flange) (Required Thickness)

1. Introduction

A corner bracket is usually provided at the connection of, for example, a deck beam and a side frame of a ship structure to reduce stress concentration and to attain smooth flow of forces. Such a bracket has sufficient strength so that no buckling takes place under usual design loads. However, it may be desirable that a bracket does not undergo buckling and/or plastic collapse until the beam with this bracket collapses under extreme loads. At the same time, it should be noticed that a bracket is the secondary one as a strength member, and it is of no use for a bracket to carry more loads after the main strength member has collapsed and lost its function. Therefore, it may be said that the necessary and sufficient conditions for a bracket are to have the thickness so that its buckling and/or plastic collapse occurs when a deck beam attains its ultimate strength. From this point of view, a method to determine the optimum thickness of a corner bracket is proposed in this report. The procedure of this method is as follows:

(1) Evaluate the plastic collapse load of a beam with effective platings,
(2) Evaluate the elastic buckling strength for a thinner bracket and the ultimate strength for a thicker bracket, either of which is considered as the limit load carrying capacity of a bracket without loosing its fundamental function, and
(3) Determine the optimum thickness of a bracket from the condition that the beam and the bracket collapses at the same time.

If the thickness of a corner bracket is determined according to the above mentioned procedure, it may be said that the bracket has necessary and sufficient thickness as to buckling or plastic strength. In practical design, the thickness of a bracket should be determined not only from buckling and/or plastic strength but also from fatigue strength. Additional care to fatigue strength should be paid.

2. Determination of the Optimum Thickness of Corner Bracket

2.1 Notations for corner bracket

In this report, a triangular corner bracket is considered with and without a flange along its free side. The lengths of supporting sides are denoted as a and b as indicated in **Fig. 1**. Supposing a bent flange as a basic example, the thickness of a flange is taken equal to that of a bracket, and its hight as:

$$b_f/t = 1.6\,a/t \cdot \sqrt{\sigma_y/E} + 4.0 \tag{1}$$

† Received on Nov. 4, 1987
* Professor
** Associate Professor, Hiroshima University

Transactions of JWRI is published by Welding Research Institute of Osaka University, Ibaraki, Osaka 567, Japan

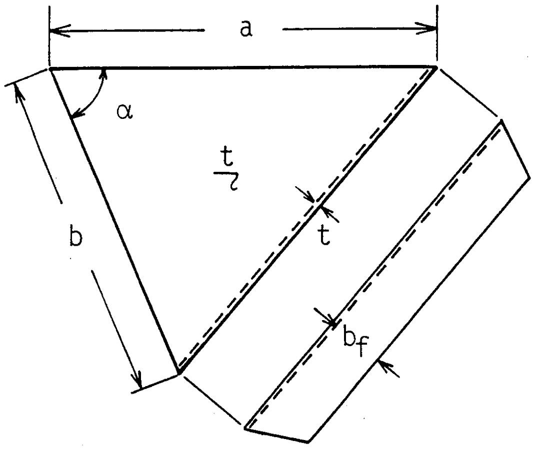

$$b_f/t = 1.6\,a/t \cdot \sqrt{\sigma_Y/E} + 4.0$$

Fig. 1 Triangular corner bracket

The above equation represents the minimum necessary hight of the flange to prevent its collapse, and is derived based on the concept of the minimum stiffness ratio against the ultimate strenth of a bracket[1, 2].

2.2 Maximum load carrying capacity of beam

First, the plastic collapse load of a beam with brackets will be derived supposing that the length and the section modulus of a beam and the geometry of a bracket are specified as shown in **Fig. 2**. The both ends of a beam are assumed to be clamped. This boundary condition may give the highest collapse load of a beam. In general, many types of loads may act along the span of a beam such as distributed and concentrated loads and their combinations. However, uniformly distributed lateral load is assumed in the following.

Figure 2(a) represents the elastic bending moment diagram of the beam with brackets subjected to uniformly distributed lateral loads, which is expressed in the following form.

$$M = q(6x^2 - 6Lx + L^2)/12 + \Delta M \tag{2}$$

where ΔM represents the influence of the brackets attached to the both ends of the beam due to change of the effective span length.

According to the magnitudes of M_t and M_c in Fig. 2(a), the first plastic hinge may be formed at the toe points of the brackets (Fig. 2(b)) or at the mid-span point (Fig. 2 (c)). In both cases, however, the final collapse mechanism shown in Fig. 2(d) is formed. The plastic collapse load for this mechanism is given as:

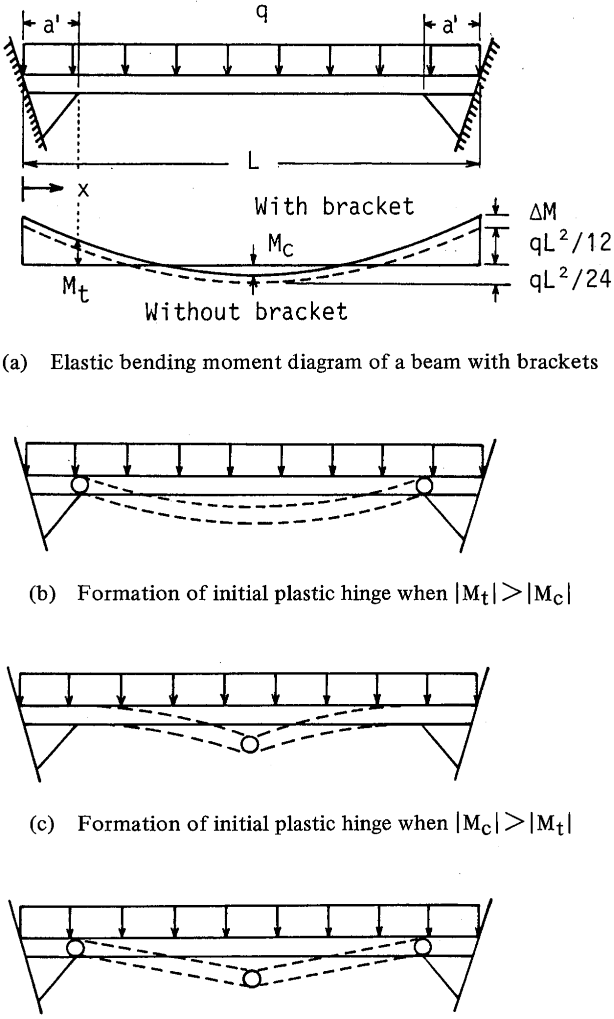

(a) Elastic bending moment diagram of a beam with brackets

(b) Formation of initial plastic hinge when $|M_t| > |M_c|$

(c) Formation of initial plastic hinge when $|M_c| > |M_t|$

(d) Plastic collapse mode

Fig. 2 Bending moment diagram and plastic collapse mode of beam

$$q_p = 16M_p/(L - 2a')^2 \tag{3}$$

where M_p is the full plastic moment of the beam.

When the lateral load expressed by Eq. (3) is acting on the beam, the bending moment at the toe point of the bracket is equal to M_p, and the shear force is;

$$V_p = 8M_p/(L - 2a') \tag{4}$$

In the actual case, a beam can carry more load than that by Eq. (3) owing to the strain hardening of the material and large deflection effect. However, at the load level above q_p, the deflection of the beam may become too large to maintain its fundamental function. So, the load expressed by Eq. (3) is regarded as the ultimate load of a beam in the following study.

2.3 Stress in bracket at the collapse of beam

Stress distribution in a bracket may depend on the rigidities of a beam, a frame and a bracket and the type of load acting on a beam. It my depend also on the detail of a structure if a frame is continuous above and below the beam. In general, a bracket may be subjected to less load if a frame is continuous. However, it is assumed not to be continuous as indicated in **Fig. 3** so that the thickness of a bracket is determined in a safe side.

Here, attention is focussed on the stress distribution along section *ff'* which intersects a beam with 45°. Normal and shear stresses on *ff'* are assumed in the following forms.

$$\sigma_y = \lambda_1 \cos \pi x/h_2 + \lambda_2 \tag{5}$$

$$\tau_{xy} = \lambda_3 \sin \pi x/h_2 - \lambda_2 (x - h_2)/h_2 \tag{6}$$

where h_2 is indicated in **Fig. A1** in Appendix. λ_1, λ_2 and λ_3 in Eqs. (5) and (6) are so determined as described in Appendix.

It is confirmed that stresses by Eqs. (5) and (6) satisfy the equilibrium condition at least along *ff'* introducing the Airy's stress function of the form[3];

$$F(x, y) = \Sigma f_i(x) g_i(y) \tag{7}$$

To check the validity of stress distributions proposed here, a series of stress analyses is performed by the finite element method. **Figure 4** shows one of the calculated results. In this case, right-angled brackets are provided at both ends of a beam of type *F* in Table 1. The side length ratio, b/a, of the bracket is varied as 1/2, 1/1 and 2/1. The side length of the bracket is taken as a = 600mm and the beam length as L = 8m. The thickness of bracket is changed from 4mm to 16mm.

In the case of $b/a = 1/2$, some differences are observed between the predicted and the calculated results. However, it may be said that the most of the stress distributions predicted by Eqs. (5) and (6) show good agreement with the calculated results.

Here, it should be noticed that the sectional forces evaluated by the proposed method are discontinuous at $x = h_1$ as indicated in Fig. 4. On the other hand, they become continuous if t_3 is taken equal to t. Also for this case, the sectional forces are evaluated and shown in **Fig. 5**, being compared with the same results in Fig. 4. It is observed that the predicted results assuming $t_3 = t$ represent the average values of the calculated results for various thicknesses by the finite element method.

In the following, the case of $t_3 \fallingdotseq t$ shall be called the

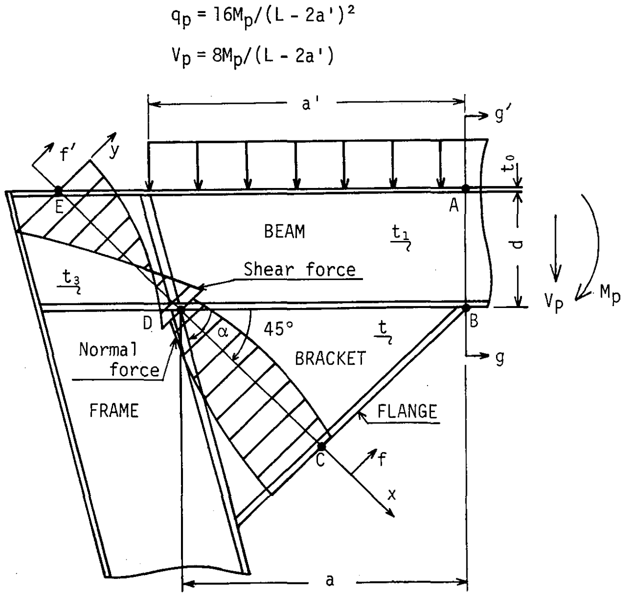

Fig. 3 Assumed distribution of normal and shear forces in bracket and frame

1st approximation and that of $t_3 = t$ the 2nd approximation.

In both cases, the mean stress in a bracket on section *ff'* in Fig. 3 is expressed as follows.

$$\sigma_m = \left(\int_{h_1}^{h} \sigma_y dx \right) / (h - h_1) = \beta(t) \tag{8}$$

where

$$\beta(t) = h_2 \lambda_1(t) (\sin \pi h/h_2 - \sin \pi h_1/h_2) / (h - h_1) + \lambda_2(t) \tag{9}$$

It should be noticed that the mean stress expressed by Eq. (8) represents the one when a beam collapses.

2.4 Limit strength of bracket

It may be said that a limit state of the fundamental function of a bracket is the beginning of reduction in its in-plane rigidity. In the case of a thin bracket, lateral deflection increases above the elastic buckling strength accompanying reduction of the in-plane rigidity. In contrast with this, in the case of a thick bracket, the in-plane rigidity decreases with local plastification due to bending caused by initial deflection, but it does not decrease so much until the ultimate strenth is attained[4, 5]. So the limit states may be the elastic buckling for a thinner bracket, and the ultimate strength state for a thicker bracket.

A series of elastic buckling analyses is performed by the finite element method, and the results are represented

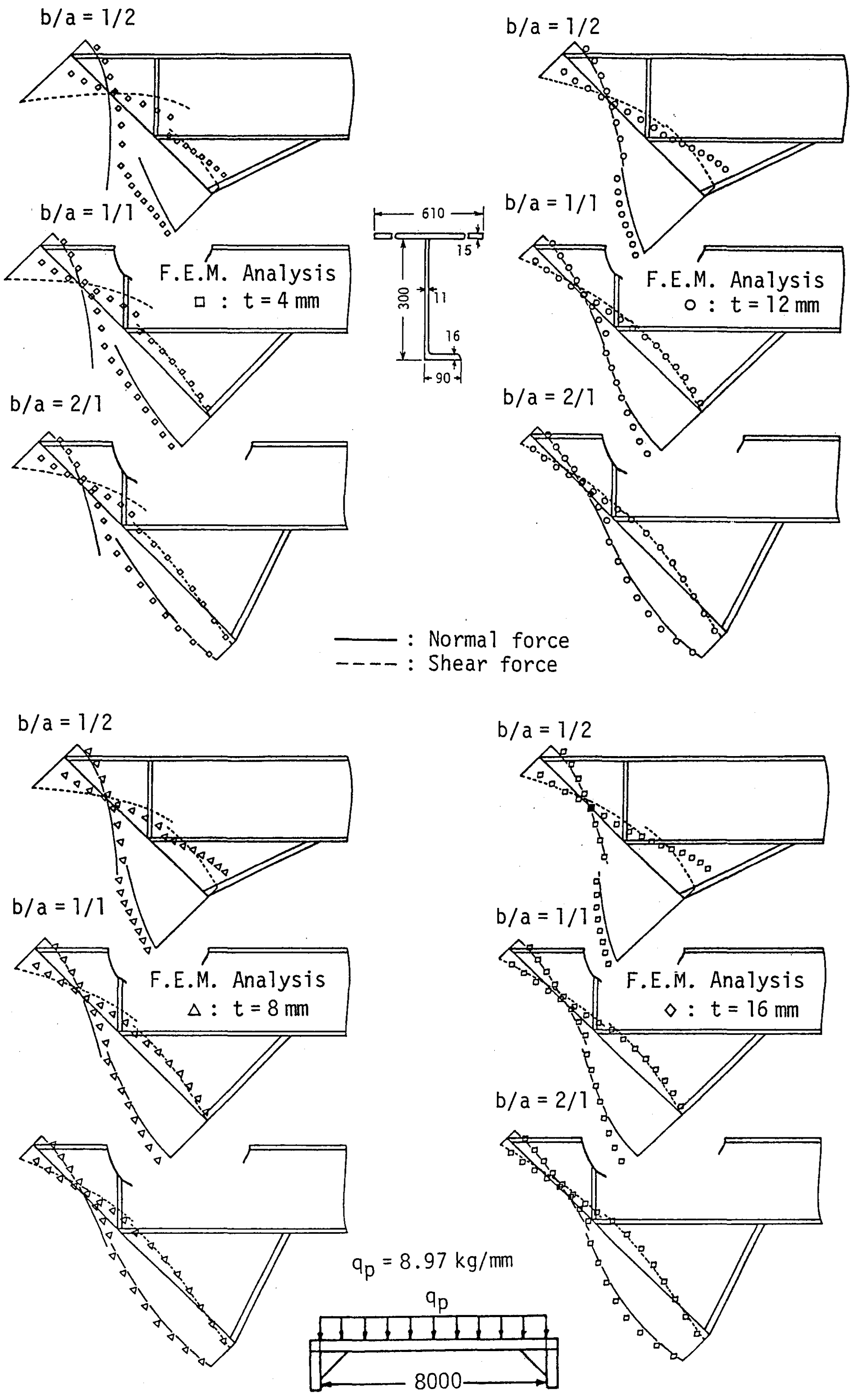

Fig. 4 Comparison of predicted and calculated sectional forces (1st approximation)

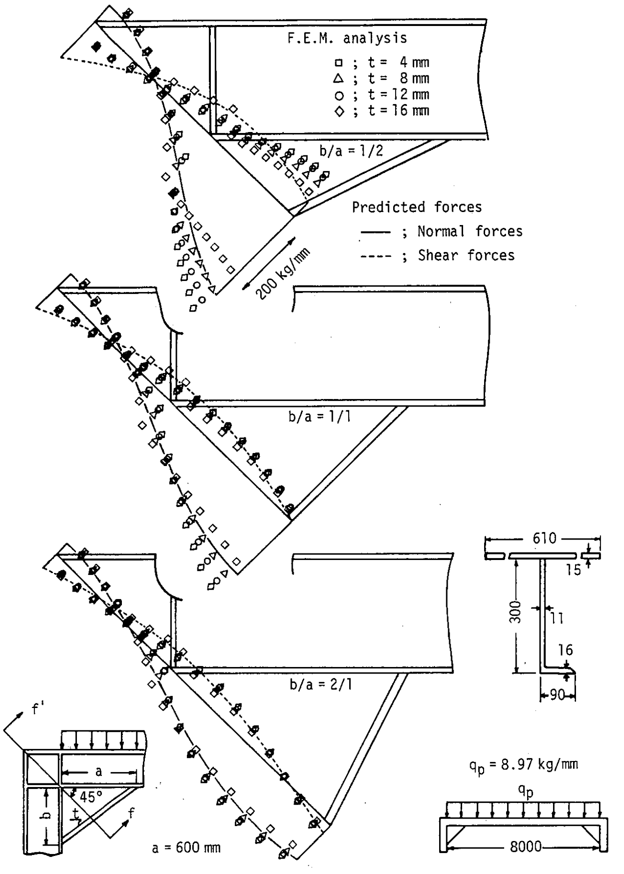

Fig. 5 Comparison of predicted and calculated sectional forces (2nd approximation)

in **Figs.** 6(a) and (b) for brackets with and without a flange, respectively. The supporting sides of a bracket are assumed to be clamped. This boundary condition was found to be appropriate comparing the calculated results with the experimental ones[4, 5]. The following two boundary conditions are applied in the analyses. In one case, linearly forced displacements are prescribed along the supporting sides, and the results are plotted by ○ in Fig. 6. In another case, load is applied through the beam and the frame to which the bracket is provided. The scatter band of the calculated results are indicated by ↕ in Fig. 6.

Based on the calculated results, the following formulae are proposed as a conservative elastic buckling strength.

$$\sigma_{cr}{}^{e} = \frac{k\pi^2 E}{12(1-\nu^2)} \left(\frac{t}{a}\right)^2 \tag{10}$$

where

$$k = \{3/(b/a - 0.2) + 1.5\}(1.0 + \cos^2\alpha)$$
$$\text{......... without a flange} \tag{11}$$

$$k = \{10/(b/a - 0.2) + 4.5\}\ \{1.87 - \cos(\alpha - 60^\circ)\}$$
$$\text{......... with a flange} \tag{12}$$

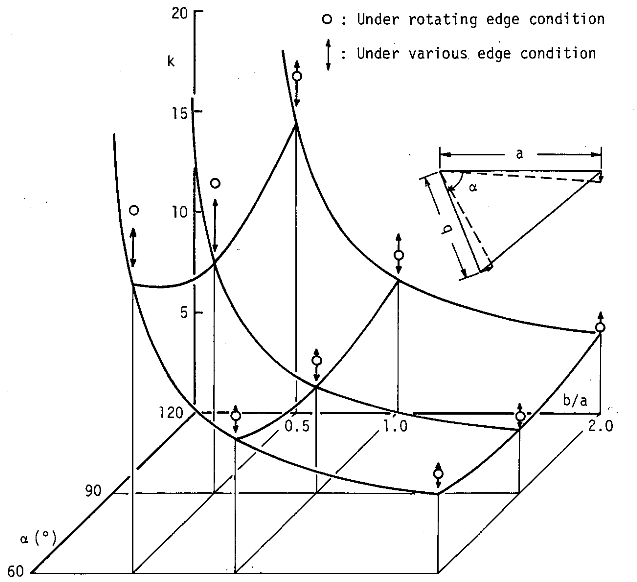

(a) Bracket without flange

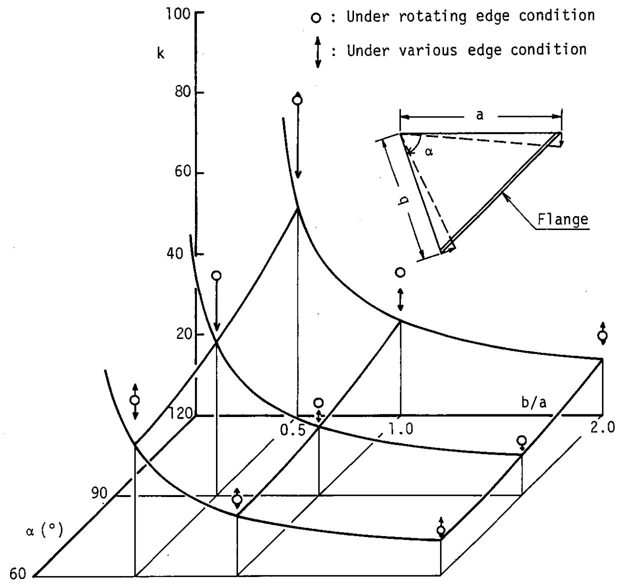

(b) Bracket with flange

Fig. 6 Elastic buckling coefficient of triangular bracket

On the other hand, the ultimate strength is also calculated performing a series of elastic-plastic large deflection analyses by the finite element method. The load is applied as the linearly forced displacements along the supporting sides. The analyses are carried out for several combinations of the side length ratio, b/a, and the angle, α, between the two supporting sides. Here, the calculated results for $b/a = 2/1$ and $\alpha = 90^\circ$ are plotted by the chain line with one dot in **Fig.** 7. The dashed line represents the elastic buckling strength and the chain line with two dots the elastic-plastic buckling strength modified by Jhonson's formula.

As mentioned above, the ultimate strength is employed as the strength at the limit state for thicker brackets. Here, the ultimate strength is rather sensitive to the initial deflection when $a/t \cdot \sqrt{\sigma_Y/E}$ is between 2.0 and 4.0. So, the ultimate strength may become lower than that indicated by the chain line with one dot in Fig. 7 in this range of $a/t \cdot \sqrt{\sigma_Y/E}$, and the following expression is proposed as a conservative ultimate strength for a thicker bracket.

$$\sigma_u/\sigma_Y = 1 - (a/\pi t)\sqrt{3(1-\nu^2)\sigma_Y/2kE} \tag{13}$$

The limit strength expressed by Eq. (13) varies linearly from $\sigma_u/\sigma_Y = 1.0$ to 0.5, and continues to the elastic buckling strength calculated by using the coefficient of Eq. (12).

The limit strengths calculated by Eqs. (10) and (13) are plotted by the solid line in Fig. 7. This seems to be too conservative comparing to the calculated results. However, it may be appropriate considering the variations of loading conditions and the influence of initial deflection in the actual cases.

2.5 Determination of the optimum thickness

The optimum thickness of a corner bracket is determined from the condition that the collapse of a beam and a bracket take place at the same time. This condition may be rephrased that avarage stresses in the bracket at the respective collapses should be equal, and is expressed as:

$$\sigma_m = \sigma_{cr}{}^e \qquad (\sigma_m \leqq \sigma_Y/2) \tag{14}$$

$$\sigma_m = \sigma_u \qquad (\sigma_Y/2 < \sigma_m) \tag{15}$$

Substituting Eqs. (8), (10) and (13) into Eqs. (14) and (15), the following equations are derived to determine the optimum thickness.

$$|\beta(t_e)|/t_e{}^2 = k\pi^2 E/12(1-\nu^2)a^2 \qquad (\sigma_m \leqq \sigma_Y/2) \tag{16}$$

$$|\beta(t_p)|/\{1-(a/\pi t_p)\cdot\sqrt{3(1-\nu^2)/2kE}\} = \sigma_Y \qquad (\sigma_Y/2 < \sigma_m) \tag{17}$$

In the calculation, t_e has to be first determined by Eq. (16). If the mean stress, σ_m, calculated by this t_e is smaller than or equal to $\sigma_Y/2$, t_e is the optimum thickness. If it is not, t_p determined by Eq. (17) is the optimum one.

3. Example Calculations and Discussions

3.1 Optimum thickness of corner bracket

A series of calculations is performed supposing that brackets are provided at both ends of the beam of which cross section is shown in **Table 1**. In the calculation, the full plastic moment of a cross section is approximated as;

$$M_p = 1.5\, Z\sigma_Y \tag{18}$$

where Z is the elastic section modulus. 1.5 in Eq. (18) corresponds to the shape factor of a rectangular cross

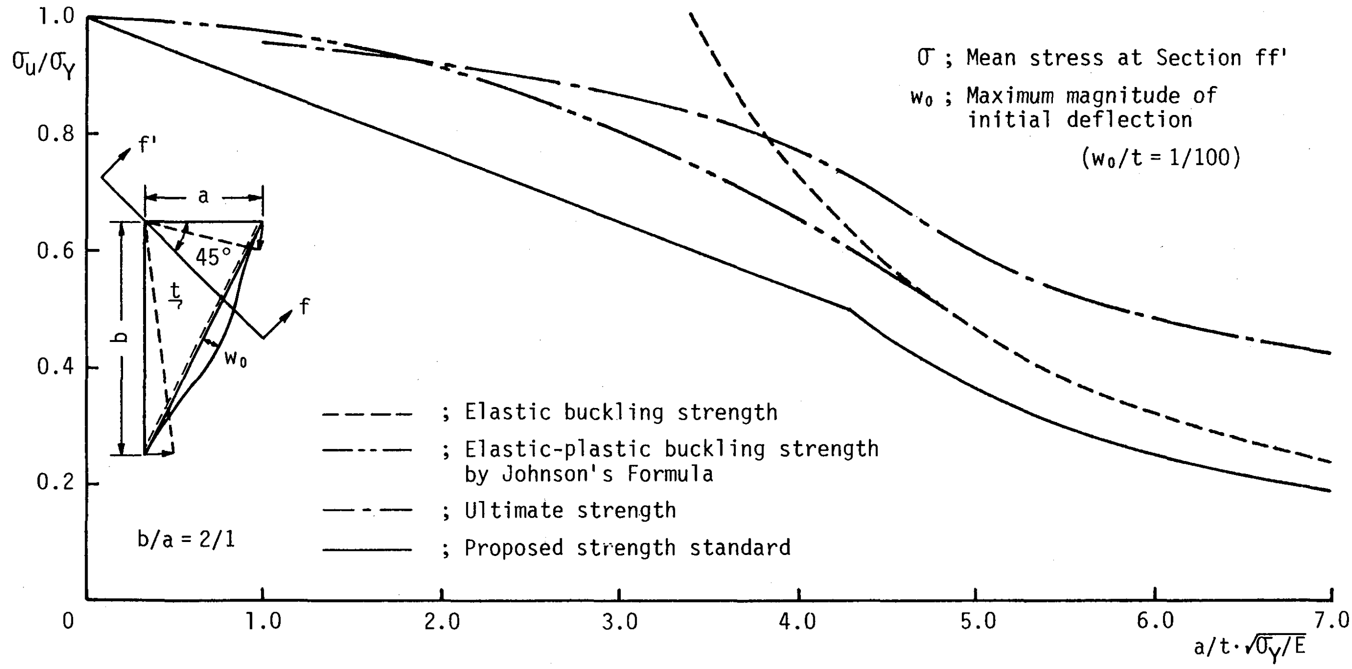

Fig. 7 Buckling and ultimate strengths of bracket with flange

section. This value may be a little larger for the cross section considered here, but it is employed to determine the optimum thickness of a bracket a little conservatively.

First, the optimum thickness is calculated employing both the 1st and the 2nd approximations for distribution of sectional forces. The results indicate that the thickness by the 2nd approximation is larger than that by the 1st one in almost all cases[2)]. So, the 2nd approximation is employed in the following, which is expected to give the optimum thickness in a conservative side.

The optimum thickness for the right-angled isosceles bracket with no flange is plotted in **Fig. 8**(a). The length of a beam is taken as 8m, and the side length to beam depth ratio, *a/d*, is varied between 1/1 and 4/1. The dashed lines represent the optimum thickness by Eq. (16), and the solid lines by Eq. (17). It may be said that the limit strength of a bracket is the elastic buckling strength when its side length is long, and is the ultimate strength when it is short. It is also said that a thicker bracket is necessary for a deeper beam because of its larger full plastic moment.

Here, ○ in Fig. 8 (a) indicates the necessary thickness specified by NK Rule[6)]. It seems that NK Rule is based on the elastic buckling criterion, and some corrosion margin may be included since the chain line representing the mean value of dashed lines in the same figure keeps a

Table 1 Beam with effective plating

Type	d (mm)	b_2 (mm)	t_1 (mm)	t_2 (mm)	t_0 (mm)	b_0 (mm)	z (cm^3)
A	100	75	7	7	10	610	72.5
B	125	90	10	10	10	610	130.0
C	150	90	12	12	15	610	230.0
D	200	90	9	14	15	610	340.0
E	250	90	12	16	15	610	540.0
F	300	90	11	16	15	610	681.0

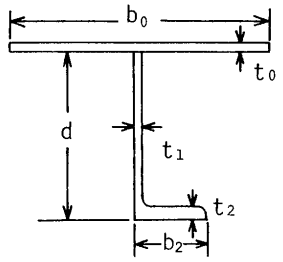

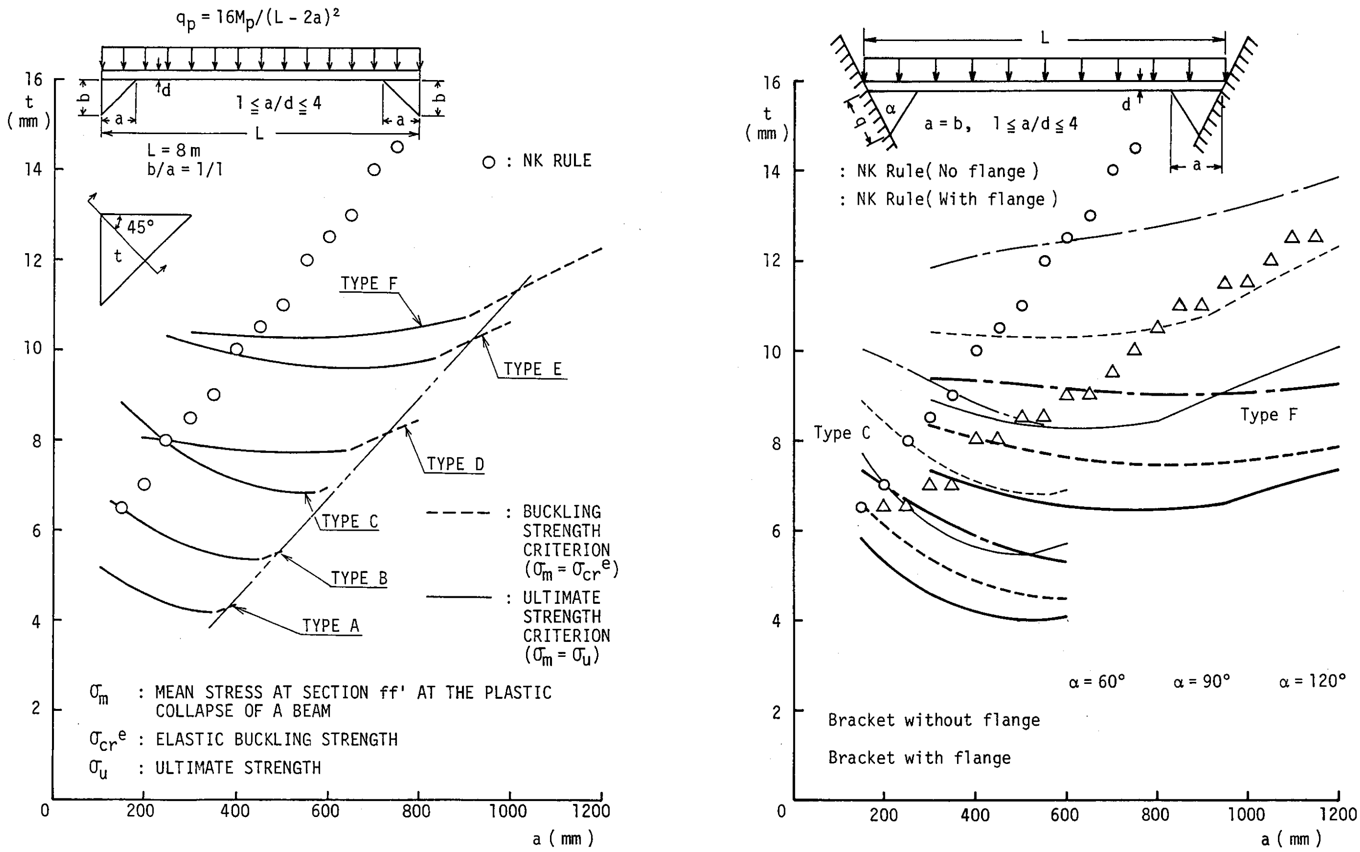

(a) Right-angled isosceles bracket with no flange (b) Isosceles bracket with and without flange

Fig. 8 Optimum thickness of triangular corner bracket nearly constant distance from O.

Figure 8 (b) shows the results for the isosceles bracket with and without a flange. In this case, the angle between the two supporting sides is taken as 60°, 90° and 120°. It is known that the optimum thickness is reduced if a flange is provided along the free side of the bracket.

3.2 Appropriateness of the proposed method

To demonstrate the accuracy of the proposed simple method, a series of elastic-plastic large deflection analyses is performed by the finite element method. The brackets and the beam are discretized into plate and beam-column elements, respectively. The both ends of the beam are assumed to be clamped, and a uniformly distributed load is applied. The relationships between lateral load and deflection of the beam are shown in **Fig. 9**. For each case of example calculation, the thickness of bracket is taken equal to the optimum one evaluated by the proposed method except the case of t = 7 mm when a = 300 mm. In these cases, plastic hinges are formed at the toe points of the brackets and the mid-span point, and the beam can carry more load than q_p evaluated by Eq. (3). In addition to this, the brackets attain their ultimate strengths soon after q_p has been attained. It may be concluded that the thickness evaluated by the proposed method is the optimum one.

Contrary to these, in the case of t = 7mm, the bracket reaches its ultimate strength before a plastic mechanism is formed in the beam. However, this is an example calculation for an extreme case when a small bracket is provided to a long beam.

4. Conclusions

In this report, a method is proposed to determine the optimum thickness of a corner bracket considering its buckling and/or plastic strength. The fundamental idea is that the bracket could collapse at the same time when the beam does. This is because that a bracket is the secondary strength member, and it is of no use for a bracket to carry more load after the beam has collapsed.

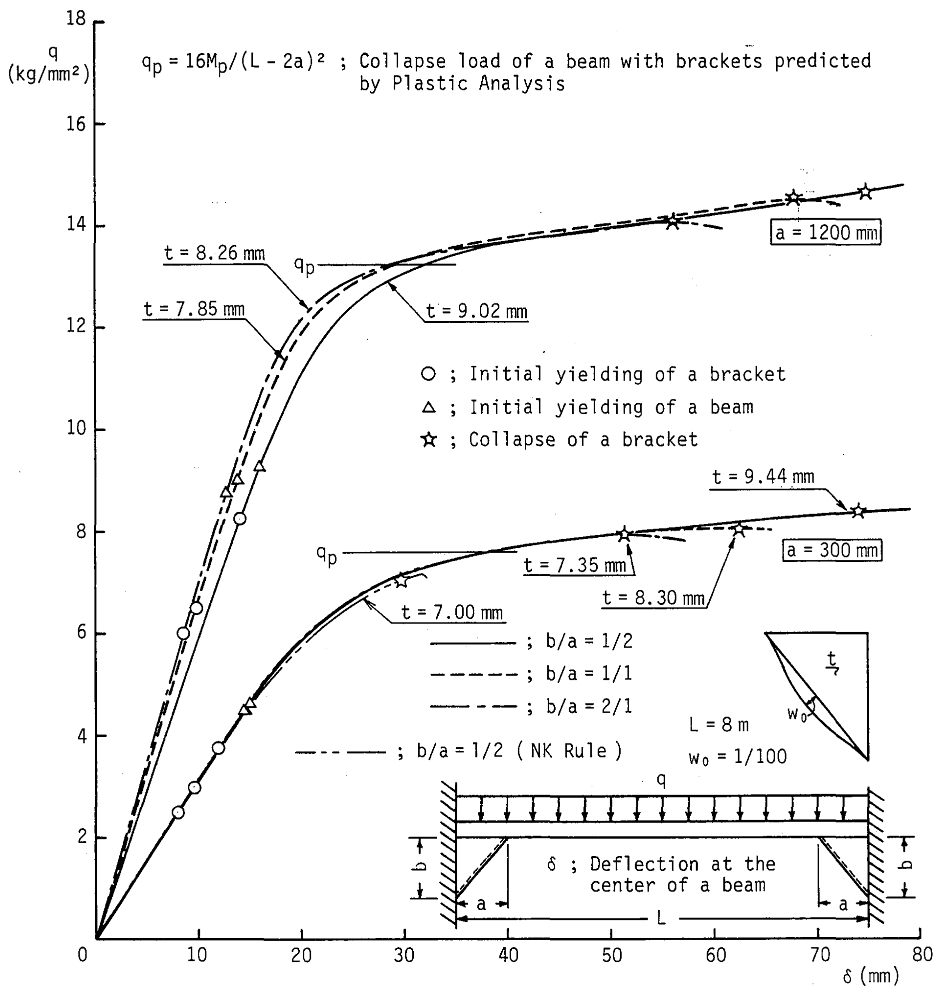

Fig. 9 Behaviour of beam with brackets subjected to uniformly distributed load

The evaluated thickness is demonstrated to be optimum by performing a series of elastic-plastic large deflection analyses by the finite element method.

In the derivation of the optimum thickness, a uniformly distributed lateral load is assumed to act along the span of a beam. If other types of loads are considered, only Eqs. (3) and (4) have to be changed. This leads to the changes in ν_2 and ν_3 in Eq. (A16) in Appendix.

References

1) Y. Ueda and T. Yao: Ultimate Strength of Compressed Stiffened Plates and Minimum Stiffness Ratio of Their Stiffeners, Eng. Structure, Vol. 5, April, 1983, pp. 97–107.
2) Y. Ueda and T. Yao: A Method to Determine Necessary Thickness of a Corner Bracket (2nd Rep.), J. Soc. Naval Arch. of Japan, Vol. 154, 1983, pp. 356–366 (in Japanese).
3) Y. Ueda and T. Yao: A Method to Determine Necessary Thickness of a Corner Bracket (1st Rep.), J. Soc. Naval Arch. of Japan, Vol. 152, 1983, pp. 286–296 (in Japanese).
4) Y. Ueda, Y. Kuramoto and T. Yao: Strength and Rigidity of Triangular Corner Bracket, J. Soc. Naval Arch. of Japan, Vol. 139, 1976, pp. 122–128 (in Japanese).
5) Y. Ueda, Y. Kuramoto and T. Yao: Effects of Initial Imperfections due to Welding on Strength and Rigidity of Triangular Corner Bracket, Trans. of JWRI, Vol. 6, No. 1, 1977, pp. 39–45.
6) Nippon Kaiji Kyokai, Roles for Classification Steel ship. 1981, p. 62 (in Japanese).

Appendix: Determination of Coefficients Representing Stress Distributions

To determine λ_1, λ_2 and λ_3 in Eqs. (5) and (6), the corner part shown in Fig. 3 is cut by sections ff' and gg'. The forces and moment acting on free-body $ABCDE$ are represented in Fig. A1. Here, the forces per unit length, N_y and N_{xy}, along section CE are given as:

$$N_y = t_3\sigma_y, \quad N_{xy} = t_3\tau_{xy} \quad \text{for } 0 \leqq x \leqq h_1 \tag{A1}$$

$$N_y = t\sigma_y, \quad N_{xy} = t\tau_{xy} \quad \text{for } h_1 < x \leqq h \tag{A2}$$

On the other hand, the concentrated forces at flanges of the beam and the bracket are obtained considering the equilibrium conditions of forces shown in **Fig. A2** as follows.

$$N_y' \cos\theta - N_{xy}' \sin\theta = S \tag{A3}$$

$$N_y' \sin\theta + N_{xy}' \cos\theta = V \fallingdotseq 0 \tag{A4}$$

where

$$N_y' = (B - t_w) \int \sigma_y dx / \cos\theta \tag{A5}$$

In the above expressions, B and t_w represent the breadth of flange and the thickness of web, respectively. Applying Eqs. (A3) and (A4) for each flange, S_u, S_l and S_f are determined as:

$$S_u = m_1\lambda_1 + m_2\lambda_2 \tag{A6}$$

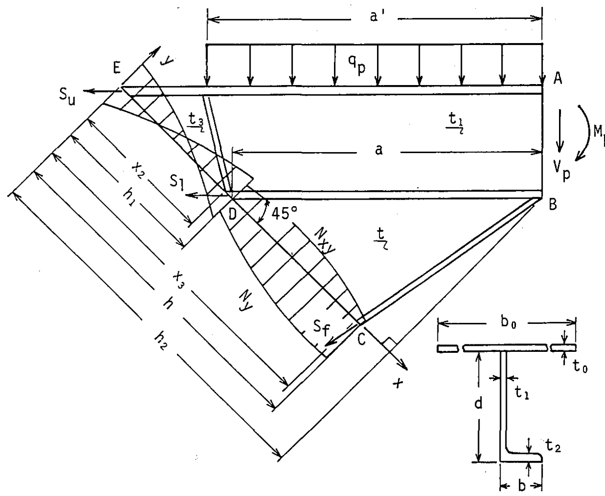

Fig. A1 Forces and moment acting on free-body

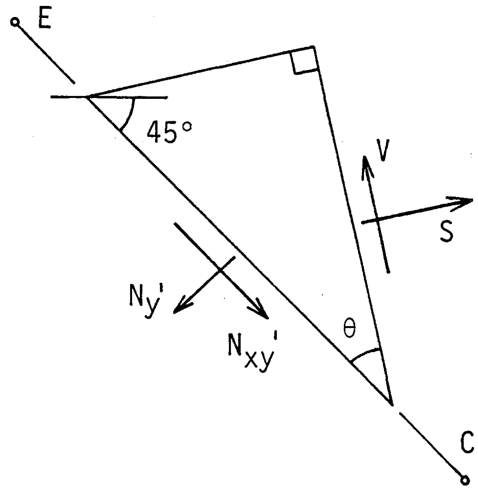

Fig. A2 Forces acting on sections of flange

$$S_l = m_3\lambda_1 + m_4\lambda_2 \tag{A7}$$

$$S_f = m_5\lambda_1 + m_6\lambda_2 \tag{A8}$$

where

$$m_1 = \sqrt{2}h_2(b_0 - t_3)\sin(\sqrt{2}\pi t_0/h_2), \quad m_2 = 2(b_0 - t_3)t_0 \tag{A9}$$

$$m_3 = \sqrt{2}h_2(b - t_3)(\sin \pi h_1/h_2 - \sin \pi x_2/h_2)/\pi, \quad m_4 = \sqrt{2}(b - t_3)(h_1 - x_2) \tag{A10}$$

$$m_5 = b_f h_2 (\sin \pi h/h_2 - \sin \pi x_3/h_2)\pi \cos\theta, \quad m_6 = b_f (h - x_3)/\cos\theta \tag{A11}$$

$$x_2 = h_1 - \sqrt{2}t_2,\ x_3 = h - t/\cos\theta,\ h_1 = \sqrt{2}(d + t_0),\ h_2 = h_1 + a/\sqrt{2},\ h = (ab\sin\alpha)/\{a - (\cos\alpha - \sin\alpha)b\},\ \cos\theta = a/\sqrt{a^2 + 2(h_2 - h)^2} \tag{A12}$$

Here, considering the equilibrium conditions of forces and moment shown in Fig. A1, the following equations are derived.

$$a_{11}\lambda_1 + a_{12}\lambda_2 + a_{13}\lambda_3 = 0 \quad \text{(A13)}$$

$$a_{21}\lambda_1 + a_{22}\lambda_2 + a_{23}\lambda_3 = v_2 M_p \quad \text{(A14)}$$

$$a_{31}\lambda_3 + a_{32}\lambda_2 = v_3 M_p \quad \text{(A15)}$$

where

$$a_{11} = m_1 + m_3 + m_5 \cos(45° - \theta) + h_2\{t_3 \sin \pi h_1/h_2 + t(\sin \pi h/h_2 - \sin \pi h_1/h_2)\}/\sqrt{2}\pi$$

$$a_{12} = m_2 + m_4 + m_6 \cos(45° - \theta) + \{h_1{}^2 t_3 + t(h^2 - h_1{}^2)\}/2\sqrt{2}h_2$$

$$a_{13} = h_2\{t_3(\cos \pi h_1/h_2 - 1) + t(\cos \pi h/h_2 - \cos \pi h_1/h_2)\}/\sqrt{2}\pi$$

$$a_{21} = m_5 \sin(\theta - 45°) + h_2\{t_3 \sin \pi h_1/h_2 + t(\sin \pi h/h_2 - \sin \pi h_1/h_2)\}/\sqrt{2}\pi$$

$$a_{22} = m_6 \sin(45° - \theta) + h_1 t_3(2 - h_1/2h_2)/\sqrt{2} + t(h - h_1)\{2 - (h + h_1)/2h_2\}/\sqrt{2}$$

$$a_{23} = -h_2\{t_3(\cos \pi h_1/h_2 - 1) + t(\cos \pi h/h_2 - \cos \pi h_1/h_2)\}/\sqrt{2}\pi \quad \text{(A16)}$$

$$a_{31} = t_0 m_1/2 + (h_1/\sqrt{2} - t_2/2)m_3 + \{(h + x_3)m_5 \cos\theta\}/2 + h_2[h_1 t_3 \sin \pi h_1/h_2 + h_2 t_3(\cos \pi h_1/h_2 - 1)/\pi + t\{h \sin \pi h/h_2 - h_1 \sin \pi h_1/h_2 + h_2(\cos \pi h/h_2 - \cos \pi h_1/h_2)/\pi\}]$$

$$a_{32} = t_0 m_2/2 + (h_1/\sqrt{2} - t_2/2)m_4 + \{(h + x_3)m_6 \cos\theta\}/2 + \{h_1{}^2 t_3 + t(h^2 - h_1{}^2)\}/2$$

$$v_2 = -8L/(L - 2a')^2$$

$$v_3 = -8\{(t_0 + d + a)L - aa' - 2a'(t_0 + d)\cos\alpha\}/(L - 2a')^2 - 1$$

$$\cos(45° - \theta) = \{a/\sqrt{2} + (h_2 - h)\}/\sqrt{a^2 + 2(h_2 - h)^2}$$

$$\sin(45° - \theta) = \{a/\sqrt{2} - (h^2 - h)\}/\sqrt{a^2 + 2(h^2 - h)^2}$$

Solving Eqs. (A13), (A14) and (A15), λ_1, λ_2 and λ_3 are determined as follows.

$$\lambda_1 = \{a_{13}a_{32}v_2 + (a_{12}a_{23} - a_{13}a_{22})v_3\}M_p/\Delta$$
$$\lambda_2 = \{-a_{31}a_{13}v_2 + (a_{21}a_{13} - a_{11}a_{23})v_3\}M_p/\Delta \quad \text{(A17)}$$
$$\lambda_3 = \{(a_{31}a_{21} - a_{11}a_{32})v_2 + (a_{11}a_{22} - a_{21}a_{12})v_3\}M_p/\Delta$$

where

$$\Delta = a_{32}(a_{21}a_{13} - a_{11}a_{23}) + a_{31}(a_{12}a_{23} - a_{22}a_{31}) \quad \text{(A18)}$$